Full characterization of modern transmission fibers for Raman amplified-based communication systems

Shifeng Jiang, Bruno Bristiel, Yves Jaouën, Philippe Gallion

GET / Telecom Paris, CNRS UMR 5141, 46 Rue Barrault, 75634 Paris, France
Tel: +33 (0)1 45 81 77 32, Fax: +33 (0)1 45 89 00 20
yves.jaouen@enst.fr

Erwan Pincemin, Sylvain Capouilliet

France Telecom, R &D, Technopôle Anticipa, 2 Avenue Pierre Marzin, 22307 Lannion , France
Tel: +33 (0)2 96 05 06 59, Fax: +33 (0)2 96 05 12 52
erwan.pincemin@orange-ftgroup.com

Abstract: Telecommunication carriers have to estimate the Raman parameters of the fibers installed on their optical transport networks in order to facilitate the design of the next generation of high bit-rate Raman amplified-based transmission systems. This paper reports a very complete characterization of the most popular modern transmission fibers in terms of Raman efficiency, noise figure and double Rayleigh backscattering crosstalk. Our experiment is based on an averaged power analysis, applied to a counter-pumped long-haul distributed fiber Raman amplifier. We evaluate as well at 40 Gb/s for these different fiber types the double Rayleigh backscattering impact in terms of Q-factor penalty for various Raman gains and RZ modulation formats with different duty cycles.

OCIS codes: (060.4510) Optical communications; (220.4830) Optical systems design; (190.5650) Raman amplification; (290.5870) Rayleigh scattering.

References and links

1. J. Bromage "Raman amplification for fiber communication systems," J. Lightwave Technol. **22**, 79-93, (2004).
2. G. P Agrawal, *Raman amplification in fiber optical communication systems* C. Headley, ed., (Elsevier Academic Press, 2005).
3. C. Rasmussen, T. Fjelde, J. Bennike, F. Liu, S. Dey, B. Mikkelsen, P. Mamyshev, P. Serbe, P. van der Wagt, Y. Akasaka, D. Harris, D. Gapontsev, V. Ivshin, and P. Reeves-Hall, "DWDM 40G transmission over trans-pacific distance (10 000 km) using CSRZ-DPSK, enhanced FEC, and all-Raman-amplified 100-km UltraWave fiber spans," J. Lightwave Technol. **22**, 203-207 (2004).
4. P. Wan and J. Conradi, "Impact of double Rayleigh backscatter noise on digital and analog systems," J. Lightwave Technol. **14**, 288-297 (1996).
5. J. Bromage, C.-H. Kim, P. J. Winzer, L. E. Nelson, R.-J. Essiambre, and R. M. Jopson, "Relative impact of multiple-path interference and amplified spontaneous emission noise on optical receiver performance," in *Proc. Optical Fiber Communication Conf.*, (2002).
6. P. J. Winzer, R.-J. Essiambre, and J. Bromage, "Combined impact of double-Rayleigh backscatter and amplified spontaneous emission on receiver noise," in *Proc. Optical Fiber Communications Conf.*, (2002); R. J. Essiambre, P. Winzer, J. Bromage, C. H. Kim, "Design of bidirectionally pumped fiber amplifiers generating double Rayleigh backscattering," IEEE Photon. Technol. Lett. **14**, 914-916 (2002).
7. M. Nissov, K. Rottwitt, H. D. Kidorf, and M. X. Ma, "Rayleigh crosstalk in long cascades of distributed unsaturated Raman amplifiers," Electron. Lett. **35**, 997–998 (1999).
8. C. Dibon, F. Boubal, P. Le Roux, E. Brandon, "Experimental validation of DRS impact on transmission system at 2.5, 10 and 40 Gbit/s," in *Proc. European Conference on Optical Communications*, (2002).
9. C. Fludger, A. Maroney, N. Jolley, R. Mears, "An analysis of the improvement in OSNR from distributed Raman amplifiers using modern transmission fibers," in *Proc. Optical Fiber Communications Conf.*, 2000.
10. F. Koch, S.A.E. Lewis, S. V. Chernikov, J. R. Taylor, "Broadband Raman gain characterization in various

#79349 - $15.00 USD Received 24 Jan 2007; revised 28 Feb 2007; accepted 5 Mar 2007; published 9 Apr 2007

optical fibers," Electron. Lett. **37**, 1437-1438 (2001).
11. J. Bromage, K. Rottwitt, and M. E. Lines, "A method to predict the Raman gain spectra of Germanosilicate fibers with arbitrary index profiles," IEEE Photon. Technol. Lett. **14**, 24-26 (2002).
12. S. H. Chang, S. K. Kim, M. J. Chu, and J. H. Lee, "Limitations in fiber Raman amplifiers imposed by Rayleigh scattering of signals," Electron. Lett. **38**, 865-866 (2002).
13. S. A. E. Lewis, S. V. Chernikov, and J. R. Taylor, "Characterization of double Rayleigh scatter noise in Raman amplifiers," IEEE Photon. Technol. Lett. **12**, 528-530 (2000).
14. R. H. Stolen and E. P. Ippen, "Raman gain in glass optical waveguides," Appl. Phys. Lett. **22**, 276-278 (1973).
15. M. O. Deventer, "Polarization properties of Rayleigh backscattering in single-mode fibers," J. Lightwave Technol. **11**, 1895-1899 (1993).
16. N. A. Olson, "Lightwave systems with optical amplifiers," J. Lightwave Technol. **7**, 1071-1082 (1989).
17. C. Martinelli, G. Charlet, L. Pierre, J. Antona, and D. Bayart, "System impairment of double-Rayleigh scattering and dependence on modulation format," in *Proc. Optical Fiber Communications Conf.*, (2003).

1. Introduction

Distributed fiber Raman amplifiers (FRAs) are known to offer a large improvement of optical signal-to-noise ratio (OSNR) with respect to usual erbium doped fiber amplifiers (EDFAs). This extra OSNR margin can be used in DWDM transmission systems to increase the channel bit-rate and/or to extend the error-free transmission distance [1-3]. In this paper, a very complete characterization of commercially available transmission fibers is reported in terms of Raman efficiency, noise figure (NF) and OSNR degradation induced by double Rayleigh backscattering (DRS). The corresponding DRS impact on the Q-factor is then evaluated at 40 Gb/s for various Raman gains.

Rayleigh scattering is an elastic process producing light scattering in all directions, resulting in signal attenuation. DRS is the phenomenon where a part of a guided light is scattered away and then back-coupled into the fiber core twice. DRS generates a detrimental in-band crosstalk, since DRS noise is a superposition of randomly delayed replicas of signal, falling in the same wavelength band. Distributed Raman amplification (DRA) increases significantly the amount of DRS noise because double Rayleigh backscattered light passes through the Raman amplifier twice and experiences gain over long fiber lengths. At high Raman gains, the DRS noise becomes the most important source of Q-factor penalty, in front of amplified spontaneous Raman scattering noise, for DRA-based transmission systems [4-8]. Consequently, full characterization of DRS generated in FRAs for different fiber types and various Raman gains is very useful for evaluating performance of these systems. In this paper, the Q-factor penalty due to DRS is calculated by means of a simple analytical tool [6] developed for RZ Gaussian pulses with different duty cycles.

In this study, a wide panel of current modern transmission fibers, used in the long-haul transport networks of telecommunication carriers, is considered: Truewave-RS^{TM}, TeraLight^{TM}, LEAF^{TM} and E-LEAF for G.655 fibers, SSMF and Allwave^{TM} for G.652 fibers and PSCF for G.654 fibers [9]. The G.655 fibers have been designed to present a lower dispersion (D) at 1550 nm (than G.652 fibers) and to ease operation of 40 Gb/s transmission systems. Their more complex index profile, characterized by a larger Germanium (GeO_2) core doping and a lower effective mode area (A_{eff}), involves strong differences in terms of Raman efficiency, noise figure, and DRS noise generation, when compared to G.652 fibers. Due to its pure silica core constitution, the PSCF has an attenuation at 1550 nm and 1455 nm lower than that of SSMF (0.18 dB/km instead of 0.20 dB/km at 1550 nm, 0.22 dB/km instead of 0.25 dB/km at 1455 nm), resulting as well in interesting features for DRA. Allwave^{TM} fiber finally is a SSMF whose water peak (at 1383 nm) has been removed, lowering advantageously the attenuation at 1383 nm (0.31 dB/km instead of 1 dB/km) but also in the region where are located Raman pumps. Our measurement results on these different fiber types constitute furthermore an interesting database for numerical simulations, supplying both Raman efficiencies and Rayleigh backscattered coefficients of the fibers the most deployed in the field.

#79349 - $15.00 USD Received 24 Jan 2007; revised 28 Feb 2007; accepted 5 Mar 2007; published 9 Apr 2007

2. Raman gain efficiency and noise figure measurements

Raman gain efficiencies have been measured using the well-known $G_{on/off}$ method [9, 10]. This technique is interesting because it permits to cancel out any inaccuracy related to spectrally dependent attenuation of components, connectors, splices and fiber under test itself. Our experimental set-up (described in Fig. 1) duplicates a realistic terrestrial DRA scheme: a constant 100-km fiber span is counter-pumped by a depolarized Raman fiber laser (RFL) at 1455 nm. The randomly polarized RFL pump light provides a polarization independent Raman gain. A 1-mW tuneable laser is used as input signal. The Raman gain spectrum is measured by means of an optical spectral analyser (OSA) with approximately 0.1 dB of accuracy. For each fiber, a reference spectrum is acquired at the amplifier output, with the pump turned "off", and a second one with the pump turned "on", all other conditions being unchanged. The difference between these two spectra gives $G_{on/off}$.

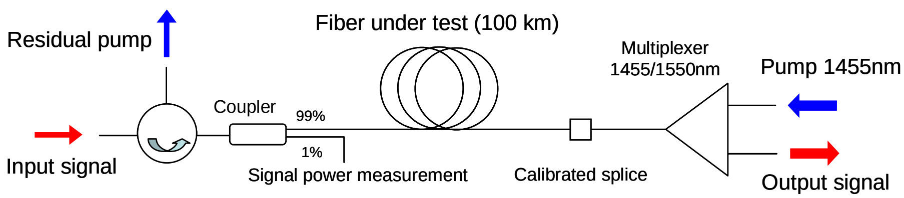

Fig 1. Experimental set-up.

The noise figure in distributed FRAs is usually referred to the equivalent noise figure (NF_{eq}) concept. It corresponds to the noise figure that a lumped amplifier placed at the end of the transmission span would need, in the absence of Raman amplification, to provide the same gain and the same noise than the distributed fiber Raman amplifier under study. As a result, the equivalent noise figure expressed in decibels can be less than zero. The NF_{eq} value is estimated here by measuring the amount of amplified spontaneous Raman scattering with the OSA and by using the well-known formula [3]:

$$NF_{eq} = \frac{1}{G_{on/off}}\left(1+\frac{P_{ASE}}{h\nu_s\, B_{OSA}}\right) \tag{1}$$

where P_{ASE}, $h\nu_s$ and B_{OSA} are the power of amplified spontaneous Raman scattering noise measured in B_{OSA}, the photon energy at signal wavelength and the OSA resolution bandwidth, respectively.

Figure 2 shows both $G_{on/off}$ and NF_{eq} at 1555 nm as a function of the pump power injected into the fiber span at 1455 nm. An attractive advantage of G.655 fibers when compared to G.652 and G.654 fibers is the need for lower P_{pump} to reach a given Raman gain. This is due to their lower mode effective area and higher GeO_2 core doping concentration [9, 11], which impacts as well their Raman gain profile inducing in particular a cancellation of the dip located at 1562 nm (see Fig. 3). Regarding noise figure results, we can note that each NF_{eq} curve presents a minimum, followed by a rapid and significant deterioration [12]. The initial NF_{eq} improvement is due to the higher increase of the signal power with respect to amplified spontaneous Raman scattering noise when the pump power rises. Deterioration results from the exacerbation of DRS generation over both the signal and amplified spontaneous Raman scattering noise. The optimal P_{pump} and $G_{on/off}$ values coincide thus with the minimum of NF_{eq} curves, which changes slightly with the fiber type. Minimum NF_{eq} of -3.25 dB and -3 dB have been measured for Truewave-RS™ and PSCF, respectively. The corresponding P_{pump} and $G_{on/off}$ are 600 mW and 29.1 dB for Truewave-RS™, and 1100 mW

#79349 - $15.00 USD Received 24 Jan 2007; revised 28 Feb 2007; accepted 5 Mar 2007; published 9 Apr 2007

and 28.8 dB for PSCF. Finally, the $G_{on/off}$ "saturation" observed on Fig. 2 (especially for the Truewave-RS^{TM} fiber) corresponds to an uncontrolled exacerbation of multi-path interference induced by Rayleigh backscattering.

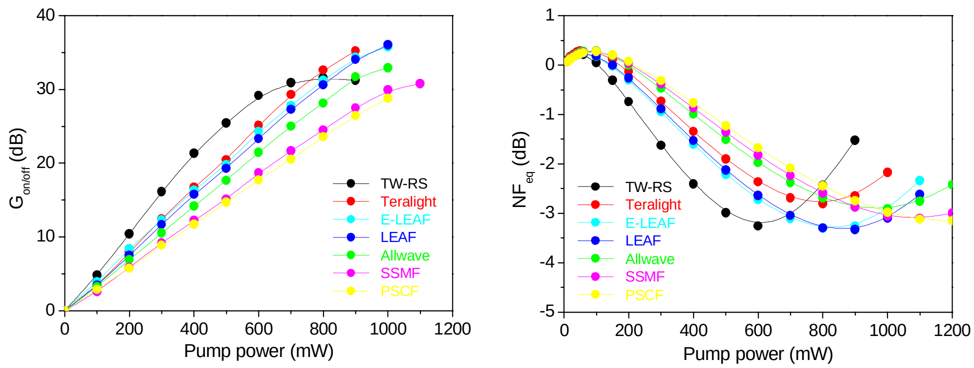

Fig 2. $G_{on/off}$ and NF_{eq} versus launched pump power at 1455 nm in the 100-km long FRAs under test (the input signal power at 1555 nm is 1 mW).

Figure 3 shows the Raman gain spectra of the fibers under test. The RFL pump and input signal powers were fixed at 700 mW and 1 mW, respectively. As previously noticed, G.655 fibers present a flatter Raman gain peak region than G.652 and G.654 fibers due to a higher GeO_2 core doping concentration [11]. This is particularly noticeable for the Truewave-RS^{TM} fiber.

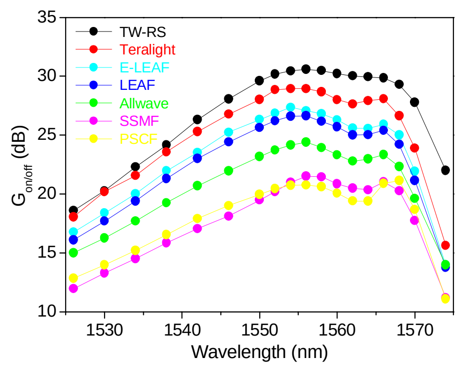

Fig 3. $G_{on/off}$ spectra of the 100-km long FRAs when the launched pump power at 1455 nm is fixed at 700 mW (the input signal power is 1 mW).

The strength of the coupling between pump and signal is determinated by the Raman gain efficiency C_R of the fiber under test, expressed in $(W.km)^{-1}$ [1,2]. The fiber Raman efficiency C_R is derived from $G_{on/off}$ (in dB) measurement owing to the following relation:

$$C_R = a \frac{G_{on/off}}{P_{pump} L_{eff}} \quad (2)$$

where $a = \ln(10)/10 \approx 0.23$, P_{pump} and $L_{eff} = [1\text{-}\exp(\text{-}\alpha_{pump} L)]/\alpha_{pump}$ are the injected pump power and the effective length of the fiber span, respectively. α_{pump} is the fiber attenuation at the pump wavelength. The estimation of Raman gain efficiencies C_R at 1555 nm for the fibers under test is summarized in the table 1: as expected, G.655 fibers present higher C_R than

#79349 - \$15.00 USD Received 24 Jan 2007; revised 28 Feb 2007; accepted 5 Mar 2007; published 9 Apr 2007

G.652 and G.654 fibers.

Table 1: Various physical parameters of the fibers under test at λ_{signal}= 1555 nm when λ_{pump}= 1455 nm.

Fiber type	1555 nm fiber parameters							
	A_{eff} μm²	D ps/nm/km	α_{pump} dB/km	C_R $W^{-1}km^{-1}$	$G_{on/off}$ dB	P_{pump} mW	$OSNR_{DRS}$ dB	k_R 10^{-8} m^{-1}
Truewave-RS™	55	4.4	0.25	0.73	21	383	40.0	8.0
TeraLight™	65	8	0.27	0.60	21	502	39.0	8.6
E-LEAF	72	4.3	0.25	0.55	21	510	39.6	8.3
LEAF™	72	3.8	0.25	0.54	21	518	40.3	7.6
Allwave™	80	17	0.24	0.44	20	582	41.5	7.2
SSMF	80	17	0.25	0.42	20	633	43.0	6.0
PSCF	80	20	0.22	0.34	18	620	46.4	4.9

3. Double Rayleigh backscattering crosstalk

DRS in fibers depends on their index profile and is thus highly correlated to their effective mode area and GeO_2 core doping. Fibers depending of various ITU recommendations are characterized by various index profiles and experience, as a result, different DRS behaviours. In our experiment, the DRS noise, travelling with the signal, is determined with the modified time-domain extinction method [13]. The optical signal to DRS noise ratio ($OSNR_{DRS}$) is defined as the signal output power from the FRA over the DRS noise power. With this technique, a direct optical measurement of $OSNR_{DRS}$ is possible. The measurement system consists of a modulated signal at 1 MHz and an optically gated receiver. Acousto-optic switches providing this modulation have an extinction ratio higher than 90 dB. The Rayleigh backscattered power is measured with the receiver sampling window out of phase with the signal, and it appears as a narrow spectral peak on the background amplified spontaneous Raman scattering level. The amplified spontaneous Raman scattering power at the signal wavelength is found using the spectral division method and subtracted from the total noise to give the DRS power. The signal output power is measured when the receiver and signal are in phase. The duty cycles of the signal and receiver are fixed at 0.5 and 0.25, respectively.

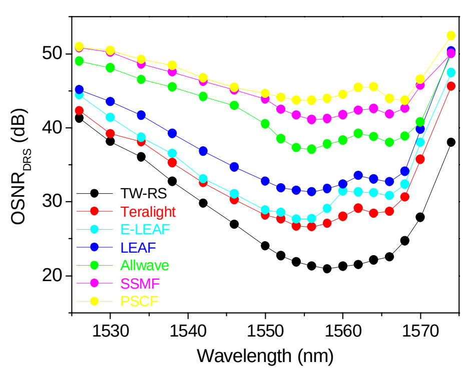

Fig 4. $OSNR_{DRS}$ spectra of the 100-km long FRAs when the launched pump power at 1455 nm is fixed at 700 mW (the input signal power is 1 mW).

Figure 4 shows the $OSNR_{DRS}$ spectra when the RFL pump and input signal powers are fixed at 700 mW and 1 mW, respectively. Note that, at lower pump powers and for fibers having both large effective area and low GeO_2 core doping, the resolution of the measurement device is not sufficient for acquiring the spectrum on the whole C-band. Indeed, with this method, it is impracticable to measure $OSNR_{DRS}$ higher than 60 dB. From Fig. 3 and Fig. 4, it

#79349 - $15.00 USD Received 24 Jan 2007; revised 28 Feb 2007; accepted 5 Mar 2007; published 9 Apr 2007

can be noticed that the higher the Raman gain, the lower $OSNR_{DRS}$. This can be explained by a greater amplification of double Rayleigh backscattering at high $G_{on/off}$, since DRS light passes through the amplifier twice and experiences higher Raman gains.

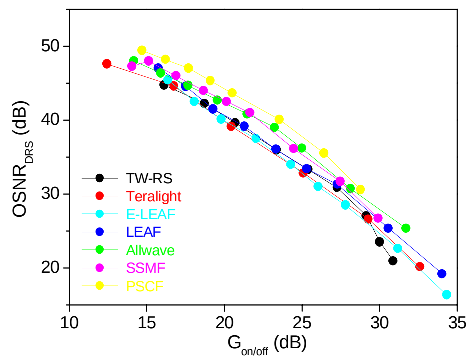

Fig 5. $OSNR_{DRBS}$ versus $G_{on/off}$ at 1555 nm when the 100-km long FRAs are counter-pumped with a RFL at 1455 nm (the input signal power is still fixed at 1 mW).

Figure 5 shows the evolution of $OSNR_{DRS}$ at 1555 nm as a function of $G_{on/off}$ for the fibers under test. As expected, when $G_{on/off}$ rises, $OSNR_{DRS}$ decreases. Moreover, fibers having small effective mode areas and high Raman efficiencies present globally a degraded $OSNR_{DRS}$ at fixed $G_{on/off}$ when compared to the other fibers. As DRS power is inversely proportional to A_{eff}^2, fibers having large A_{eff} present improved $OSNR_{DRS}$ [13]. When comparing on Fig. 5 Truewave-RS™ to PSCF in terms of $OSNR_{DRS}$ for a fixed Raman gain of 20 dB, a shift of nearly 3.5 dB is shown. This difference is due to the A_{eff}^2 ratio between the two fibers: the theory foresees a difference of 10.log $(80^2/55^2) = 3.2$ dB in good agreement with our measurement. As a result, G.655 fibers, with higher C_R and substantially lower A_{eff}, present lower $OSNR_{DRB}$ than G.652 and G.654 fibers.

In the small-signal regime (i.e. neglecting the pump depletion), the Rayleigh backscattered coefficient k_R of each fiber under test can be straightforwardly deducted from $OSNR_{DRS}$ (in dB) measurement owing to the formula given underneath [7]:

$$OSNR_{DRS} = -10 \log\left(k_R^2 \int_o^L \int_o^z \frac{G^2(z)}{G^2(y)}\, dy\, dz \right) \tag{3}$$

where L is the fiber span length and $G(z)$ is the amplifier gain along the span ($G(z)=P_s(z)/P_s(0)$ where P_s is the signal power). When the pump depletion is negligible, the analytic expression of the counter-pumped amplifier gain can be found as [1] :

$$G(z) = \exp\left[C_R P_{pump}(L)\, e^{-\alpha_{pump} L} \left(e^{\alpha_{pump} z} - 1 \right) / \alpha_{pump} - \alpha_{signal} z \right] \tag{4}$$

Table 1 summarizes the values of Rayleigh backscattered coefficients k_R at 1555 nm, when the losses of the 100-km long fiber spans under test are exactly compensated by DRA. The corresponding $G_{on/off}$, P_{pump}, $OSNR_{DRS}$ values (at transparency) are also given in the table 1. G.655 fibers are characterized by k_R values in the range 7.6-8.6 10^{-8} m^{-1}, whereas G.652 and G.654 fibers have lower k_R (in the range 4.9-7.2 10^{-8} m^{-1}). GeO_2 doping, added in the silica core of fibers to increase the refractive index, results not only in a substantial improvement of the fiber Raman gain efficiency C_R [11], but contributes also to increase k_R and thus to degrade $OSNR_{DRS}$.

#79349 - $15.00 USD Received 24 Jan 2007; revised 28 Feb 2007; accepted 5 Mar 2007; published 9 Apr 2007

4. Q-factor penalty induced by double Rayleigh backscattering noise

DRS noise is a key issue in high bit-rate Raman-based transmission systems because it results in OSNR degradation. Consequently, to design properly future DRA-based transmission systems, it is essential to evaluate Q-factor penalties induced by DRS noise, for both various fiber types and Raman gains [3-8]. Actually, a continuous wave approach is widely adopted: the total beat noise variance is obtained by substituting the optical power corresponding to the signal-ASE beat noise (by analogy with EDFA, the amplified spontaneous Raman scattering is now referred as ASE noise) with the power resulting from the signal-DRS beating. Unfortunately, this approach neither accounts for the influence of narrow-band filtering of signal pulses on beat noise, nor for the different spectral distribution of ASE and DRS noise. Indeed, ASE can be considered as "white" noise in the range of the signal bandwidth at the opposite of "colored" (frequency dependant) DRS noise. Expressions of both signal-ASE and signal-DRS beat noise variances ($\sigma^2_{s\text{-}ASE}$ and $\sigma^2_{s\text{-}DRS}$) have been proposed in reference [6], where the optical and electrical filters and the signal pulses are all assumed to be Gaussian:

$$\sigma^2_{s-ASE} = \left(\frac{e}{h\nu_s}\right)^2 . \frac{4.P_1.N_{ASE}.B_{elec}}{\sqrt{1+2\frac{B_s^2}{B_{opt}^2}+\frac{4B_{elec}^2}{B_{opt}^2}\left[1+\frac{B_s^2}{B_{opt}^2}\right]} . \sqrt{1+\frac{B_s^2}{4B_{elec}^2}+\frac{B_s^2}{B_{opt}^2}}} \tag{5a}$$

$$\sigma^2_{s-DRS} = \left(\frac{e}{h\nu_s}\right)^2 . \frac{2P_1.P_{DRS//}}{\sqrt{1+\frac{B_s^2}{B_{opt}^2}} . \sqrt{1+\frac{B_s^2}{B_{opt}^2}+\frac{B_s^2}{2B_{elec}^2}} . \sqrt{1+\frac{B_s^2}{B_{opt}^2}+\frac{B_s^2}{4B_{elec}^2}}} \tag{5b}$$

where N_{ASE} is the power spectral density of the ASE noise, $P_{DRS//}$ is the co-polarized DRS noise power measured before optical filtering, P_1 denotes the peak optical pulse power before optical filtering as well. B_s, B_{opt}, and B_{elec} correspond to the signal, optical and electrical filter equivalent square bandwidths, respectively. Note that in the limit of broadband optical filtering and quasi continuous wave signaling ($B_s << B_{elec} << B_{opt}$) the Eq. (5) simplify to the well-known expressions [6,16]:

$$\sigma^2_{s-ASE} = \left(\frac{e}{h\nu_s}\right)^2 .4.P_1.N_{ASE}.B_{elec} \tag{6a}$$

$$\sigma^2_{s-DRS} = \left(\frac{e}{h\nu_s}\right)^2 .\,2P_1.P_{DRS//} \tag{6b}$$

The parameters P_1, N_{ASE} and P_{DRS} are related to measured $OSNR_{ASE}$ (optical signal to ASE noise ratio) and $OSNR_{DRS}$ by:

$$OSNR_{ASE} = \frac{P_s}{2N_{ASE}.B_{OSA}} = \frac{R_s.P_1}{2N_{ASE}.4.B_S.B_{OSA}} \tag{7a}$$

$$OSNR_{DRS} = \frac{P_s}{P_{DRS}^{TOTAL}} = \frac{R_s.P_1}{\frac{9}{5}.P_{DRS//}.4.B_S} \tag{7b}$$

P_s is the average signal power (still before optical filtering), B_{OSA} is the OSA resolution and R_s is the bit rate. As pulses are Gaussian, the average signal power P_s is linked to P_1, R_s and B_s by the relation:

#79349 - $15.00 USD Received 24 Jan 2007; revised 28 Feb 2007; accepted 5 Mar 2007; published 9 Apr 2007

$$P_s = \frac{R_s.P_1}{4B_s} \tag{8}$$

We note P_{DRS}^{TOTAL} as the total DRS noise power (measured with the OSA owing to the modified time-domain extinction method), the sum of contributions of the DRS noise over the two principal polarization axis of the fiber. P_{DRS}^{TOTAL} is linked to the DRS noise power $P_{DRS//}$, orientated in the same polarization than the signal, by the following equation:

$$P_{DRS\,//} = \frac{5}{9} P_{DRS}^{TOTAL} \tag{9}$$

Indeed, it has been shown [3,15] that, in long standard single-mode fibers, the DRS noise power beating with the signal is 5/9 of the total DRS noise power due to the polarization rotation of the double reflected signal relative to the original signal.

$OSNR_{ASE}$ and $OSNR_{DRS}$ are then measured at 1555 nm for various Raman gains, by means of the time-domain extinction method previously described [13], for a typical terrestrial Raman distributed amplification span constituted of 100-km of each fiber under test (1 mW of signal power is injected into the spans). If we note $\sigma^2_{shottky}$ as the variance of the shot noise, the Q-factor at the transmission end is defined by the relation:

$$Q_{dB} = 20.\log\left[\frac{e}{h\nu_s}.\frac{P_1}{\left(\sigma^2_{Schottky} + \sigma^2_{s-ASE} + \sigma^2_{s-DRS}\right)^{1/2}}\right] \tag{9}$$

The Q-factor at the emission side is supposed to be shot noise-limited. As the corresponding Q-factor reference is noted Q_o, the Q-factor penalty ΔQ after insertion of the FRA between the transmitter and the receiver is then defined as $\Delta Q = Q_o - Q_{dB}$.

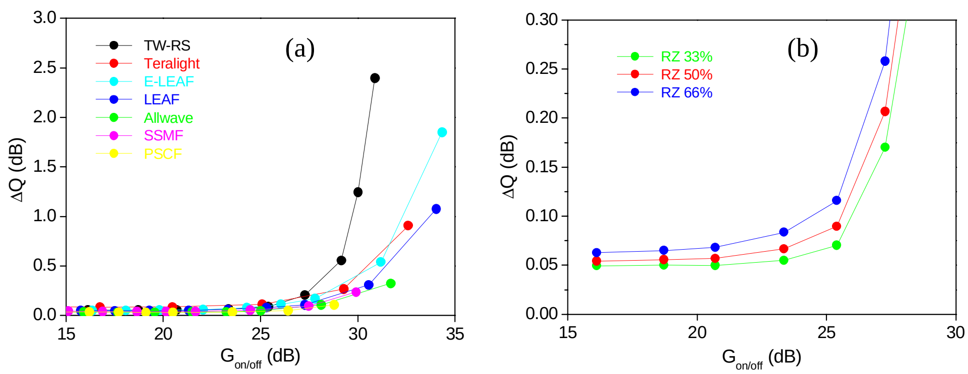

Fig. 6. (a). Q-factor penalties versus $G_{on/off}$ at 1555 nm for one 100-km long amplification span of the various fibers under test and 40 Gb/s RZ 50% Gaussian pulses; (b) Q-factor penalties versus $G_{on/off}$ at 1555 nm, for one 100-km long amplification span of Truewave-RS^{TM} fiber and for 40 Gb/s RZ 3%,RZ 50% and RZ 66% Gaussian pulses.

Figure 6(a) depicts the evolution of the Q-factor penalty at 1555 nm versus the Raman gain for RZ 50% Gaussian pulses and for the various fiber types (the average power at the amplifier input is still equal to 1 mW). R_s, B_s, B_{opt} and B_{elec} are respectively set at 40 Gbit/s, 37.6 GHz, 79.8 GHz and 18.8 GHz. B_s is linked to the temporal full width half maximum (FWHM) Δt_s of the RZ 50% Gaussian pulses by the formula given underneath:

#79349 - $15.00 USD Received 24 Jan 2007; revised 28 Feb 2007; accepted 5 Mar 2007; published 9 Apr 2007

$$B_s = \frac{1}{\Delta t_s}\sqrt{\frac{\ln(2)}{\pi}} \tag{10}$$

The FWHM bandwidth $\Delta\nu_{opt}$ of the optical filter used in the receiver is fixed at 0.6 nm (or 75 GHz). B_{opt} is then straightforwardly deduced from $\Delta\nu_{opt}$ owing to the following equation:

$$B_{opt} = \frac{1}{2}\sqrt{\frac{\pi}{\ln(2)}}\,\Delta\nu_{opt} \tag{11}$$

We made also the assumption that the FWHM bandwidth $\Delta\nu_{elec}$ of the electrical filter implemented in the receiver is equal to the FWHM bandwidth of the signal. Therefore, B_{elec} is related to B_s by:

$$B_{elec} = \frac{B_s}{2} \tag{12}$$

At gains lower than 25 dB, the Q-factor penalties are negligible for the different fiber types considered here. In the high gain regime (in the range 25-30 dB), degraded Q-factors are observed: this degradation is mainly due to the OSNR deterioration related to DRS exacerbation. At very high Raman gains (greater than 30 dB), the Q-factor collapse is dramatically high whatever the fiber type: it can be explained by the severe decrease of the $OSNR_{ASE}$ and $OSNR_{DRS}$ values, well-observed on both Fig. 2 (NF_{eq} vs. $G_{on/off}$ curve) and Fig. 5 ($OSNR_{DRS}$ vs. $G_{on/off}$ curve). As a result, by considering furthermore that many amplification spans are concatenated in a real transmission system (which enhances the impact of DRS noise), Raman gains used in DWDM communication systems are often limited to values that do not compensate the overall span attenuation. This is particularly true in the case of G.655 fibers with especially high Raman efficiency.

Finally, it has been shown in [17] that the contribution of DRS and ASE noises to the total electrical noise depends on the modulation format. Indeed, as shown in formulas (5), the beat noise variances $\sigma^2_{s\text{-}ASE}$ and $\sigma^2_{s\text{-}DRS}$ are strongly correlated to the optical and electrical filter bandwidths, whose the optimization depends on the modulation formats. Figure 6(b) shows the Q-factor penalty at 1555 nm as a function of the Raman gain for the Truewave-RS™ fiber and for RZ 33%, RZ 50% and RZ 66% Gaussian pulses. R_s is fixed at 40 Gbit/s. B_s, B_{opt} and B_{elec} (obtained using the method described above) are respectively set at 56.36 GHz, 106.44 GHz and 28.18 GHz for RZ 33% - 37.6 GHz, 79.8 GHz and 18.8 GHz for RZ 50% - 28.18 GHz, 79.8 GHz and 14.1 GHz for RZ 66%. Note that we have taken the same optical filter bandwidth for RZ 50% and RZ 66% modulation formats because their respective optimal filter bandwidths are in fact very close to each other. We observe that the lower the pulse duty cycle, the lower the Q-factor penalties induced by ASE and DRS noise are. Indeed, the higher the pulse peak power, the more resilient the pulses to the accumulation of both ASE and DRS. Furthermore, we have represented on Fig. 7 the ratio $\sigma^2_{s\text{-}ASE}/\sigma^2_{s\text{-}DRS}$ as a function of B_{elec} (at B_{opt} = constant) or B_{opt} (at B_{elec} = constant) for RZ 33%, RZ 50% and RZ 66% Gaussian pulses. What can be noticed first is that the ASE noise becomes predominant at high optical or electrical bandwidths. It makes sense since the ASE noise contribution enhances while the DRS noise remains almost constant with increasing bandwidths. On the other hand, when both the optical and electrical filter bandwidths decrease, the DRS noise becomes the main source of impairment since ASE noise is largely suppressed by filtering. Finally, when considering influence of the pulse duty cycle, one can note that the lower the pulse duty cycle, the higher the pulse spectral occupancy, the higher the filter bandwidth, the more important the impact of ASE noise is when compared to DRS noise.

#79349 - $15.00 USD Received 24 Jan 2007; revised 28 Feb 2007; accepted 5 Mar 2007; published 9 Apr 2007

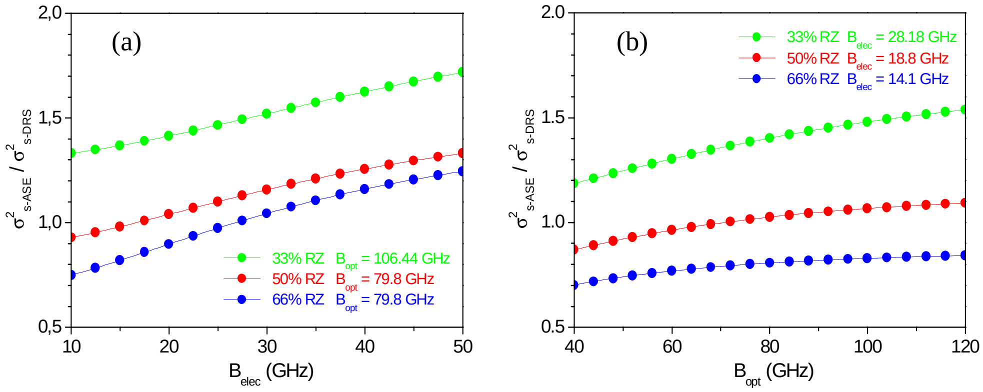

Fig. 7. $\sigma^2_{s\text{-}ASE}/\sigma^2_{s\text{-}DRS}$ ratio evolution for RZ 33%, RZ 50% and RZ 66% Gaussian pulses: (a) versus B_{elec} (at constant B_{elec}), (b) versus B_{opt} (at constant B_{elec}).

5. Conclusion

Full characterization of achievable Raman gain and crosstalk due to amplified spontaneous Raman scattering and double Rayleigh backscattering has been performed for the most popular modern transmission fibers in a typical terrestrial distributed fiber Raman amplifier. When operating at the same Raman gain, G.652 and G.654 fibers are less sensitive to DRS crosstalk than G.655 fibers, even if their Raman gain spectral flatness is lower and the required pump power to reach this Raman gain is higher. Our extensive measurement set of fiber Raman parameters constitutes a very complete database for people involved in transmission system design activities, providing both Raman gain efficiencies and Rayleigh backscattered coefficients of the fibers the most deployed in the field. Furthermore, the interesting analytical analysis developed here permits to assess the Q-factor transmission penalties of diverse RZ modulation formats (with different duty cycles) due to the various noise sources of a fiber Raman amplifier, based on the implementation of the most recent transmission fibers.

#79349 - $15.00 USD Received 24 Jan 2007; revised 28 Feb 2007; accepted 5 Mar 2007; published 9 Apr 2007